JOURNAL OF CATALYSIS 39, 412–418 (1975)

The Catalytic Reduction of Nitrous Oxide by Carbon Monoxide over Tin(IV) Oxide

M. J. FULLER AND M. E. WARWICK

Tin Research Institute, Greenford, Middlesex UB6 7AQ, England

Received November 11, 1974; revised April 3, 1975

The kinetics of the reaction $CO + N_2O \rightarrow CO_2 + N_2$ have been investigated at 190–220°C on 450°C-activated SnO_2 gel using a differential flow reactor. The steady state kinetics are adequately represented by the empirical relationship:

$$\text{rate} = A \exp(-E/RT) p_{CO}^{0.2} p_{N_2O}^{0.5},$$

with $E = 24.3$ kcal mole^{-1} and no product inhibition by CO_2 or N_2.

Evidence is presented indicating that the reaction occurs principally by catalyst redox involving CO chemisorption, CO_2 desorption via lattice oxygen abstraction, and reoxidation of the catalyst by N_2O, the last being the rate determining step. The extent of reduction of SnO_2 after attainment of steady state in CO–N_2O reactant mixtures can be estimated by monitoring evolved N_2 during dynamic gas titration of the catalyst with N_2O. Expressed as a function of the degree of reduction (θ), the kinetics equation becomes:

$$\text{rate} \propto p_{CO}^{0.0} p_{N_2O}^{0.8} \theta.$$

INTRODUCTION

Although the catalytic reduction of N_2O by CO has been studied on several simple (*1–3*) and mixed (*4,5*) oxide systems over the years, the observation by Shelef and Otto (*6*) that the low-temperature reduction of NO to N_2 by CO over several oxide systems occurs principally through the intermediate formation of N_2O renders this reaction of relevance to the current interest in the removal of NO_x from automotive exhausts by catalytic reduction with CO.

Studies on simple oxides of Cu (*1,2*) and Zn (*3*) have indicated that the CO–N_2O reaction on these occurs by reduction of the catalysts by CO followed by their reoxidation with N_2O. On the other hand, Leech and Peters (*5*) have postulated a mechanism involving surface reaction of chemisorbed CO and N_2O species for this reaction on chromium-promoted iron oxide, and the reaction on *p*- and *n*-type cobalt ferrite catalysts has been explained in terms of dissociative chemisorption of N_2O to give oxygen atoms, followed by their reaction with CO (*4*).

As part of a general investigation into the catalytic oxidation of CO by oxygen (*7–9*) and nitrogen oxides (*10*) on tin oxide-based gel catalysts, we report here details of a kinetics and mechanistic study of the CO–N_2O reaction on tin(IV) oxide gel.

METHODS

Catalyst Preparation and Characterization

The preparation of the tin(IV) oxide gel catalyst and its physical characterization have been described previously (*8*).

Catalytic Studies and Gas Analyses

The apparatus for the steady state kinetics studies and gases used were as previously reported (*8*) except that activated molecular sieve type 5A pellets were used exclusively for drying the feed gases, and

the N_2O ($\geq 99.8\%$) was B.O.C. medical grade.

A "microreactor" was used for the experiments described in the Redox Studies section. This consisted of an essentially similar apparatus to that used for the steady state kinetics studies with the omission of the gas preheater–premixer. In addition, this system contained a manifold of 3-way stopcocks whereby the reactant and carrier gases could be passed, either singly or in any required combination, through the catalyst bed. All connections to the reactor were by narrow bore glass tubing, and the total volume from the manifold to the gas chromatograph sample valve(s) was less than 5 cm^3. A gas collector was connected to the outlet side of the GC sample valve(s) by a 3-way capillary stopcock. This consisted of a 100 cm^3 gas burette and mercury leveling bottle, such that a known volume of gas could be collected by mercury displacement and then forced back through the GC sample valve(s) for analysis. This arrangement permitted both continuous on-line and batch analyses. Unless otherwise stated 36–72 B.S.S. mesh (0.42–0.21 mm) catalyst granules were used, and thermal activation was carried out in the reactor.

The reactant and product gases were separated and analyzed using Perkin-Elmer F11 gas chromatographs with hot wire detectors and He carrier gas. Columns used were molecular sieve type 5A at 100°C (for N_2 and CO) followed by temperature programming up to 350°C (for N_2O and, nonquantitatively, CO_2), and Porapak Q at 50 or 70°C for N_2O and CO_2.

RESULTS

Steady State Kinetics Studies

The attainment of steady state during the CO–N_2O reaction on 450°C-activated SnO_2 gel was found to be much more rapid than that previously observed for the air oxidation of CO on this catalyst (*8*). In general, essentially steady state conditions were achieved with a 1 g bed after 3–4 hr contact with the CO–N_2O reactant gases at ~200°C although a period of at least 18 hr was allowed before attempting a kinetics run, and all data presented in this section refer to the steady state condition.

As was observed during the low-temperature (<250°C) oxidation of CO on this catalyst (*8*), the attainment of steady state is accompanied by a darkening in color of the catalyst granules from yellow to dark brown-black. This is attributable to lattice oxygen deficiences in the steady state catalysts, which are shown to exist in a partially reduced form (see below), and a similar effect is observed during the low-temperature oxidation of hydrogen on this catalyst (*11*).

No evidence of carbon deposition was observed during these CO–N_2O studies. This was checked by subjecting well-flushed (with Ar at 250°C) steady state catalysts to an air stream at temperatures up to 500°C. Evolution of CO_2 did not accompany the reoxidation (lightening in color) of the catalyst.

Neither reaction of CO with N_2O on the empty reactor nor decomposition of N_2O in the absence of CO on freshly activated SnO_2 was detected at the reaction temperatures used during this study. Furthermore, in no instance was NO detected in the product gases during the catalysis studies, indicating that the reaction:

$$N_2O + CO_2 \rightarrow 2NO + CO,$$

does not occur to any significant extent under the experimental conditions used.

The effect on kinetics of external (mass transfer) diffusion was found to be negligible at the space velocity (~15,000 hr^{-1}) and temperatures (190–220°C) used in the kinetics experiments. By varying the space velocity of a constant composition gas mixture through a 1.0 g bed at 220°C, no appreciable change in percentage of N_2O

reduction was observed, at least in the space velocity range 5000–22,000 hr^{-1}.

The effect of internal (pore) diffusion was investigated again at 220°C by measuring the rate of reaction under identical feed and flow rate conditions for 1.0 g beds of (a) 0.10–0.21 mm (72–150 B.S.S. mesh), (b) 0.21–0.42 mm (36–72 B.S.S. mesh), and (c) 0.42–0.78 mm (20–36 B.S.S. mesh) catalyst granules. The reaction rates on each catalyst bed were essentially the same, showing evidence of the absence of pore diffusion control.

The effect on the rate of the CO–N_2O reaction at 200°C of adding product gases was investigated by replacing some of the Ar diluent in the CO–N_2O–Ar reaction mixtures with CO_2 or N_2. In neither case did the added products significantly alter the observed reaction rates, indicating the absence of product inhibition.

The effects of CO and N_2O concentrations on the rates of reaction at 190, 200, 210 and 220°C are shown in Figs. 1 and 2, respectively. These results were obtained under essentially differential conditions, and the large majority of data points in Figs. 1 and 2 correspond to overall conversions of $< 10\%$ with respect to both N_2O and CO.

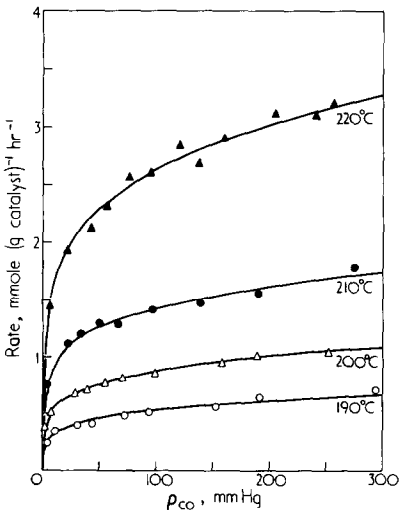

FIG. 1. Effect of p_{CO} on CO–N_2O reaction rate on 450°C-activated SnO_2. CO–N_2O–Ar feed at 100 ± 2 cm^3 min^{-1} and constant p_{N_2O} (100 mm Hg) through 1.0 g bed: (—) plots for rate $= k_1 p_{CO}^{0.2}$ for best-fit values of k_1 at each temperature.

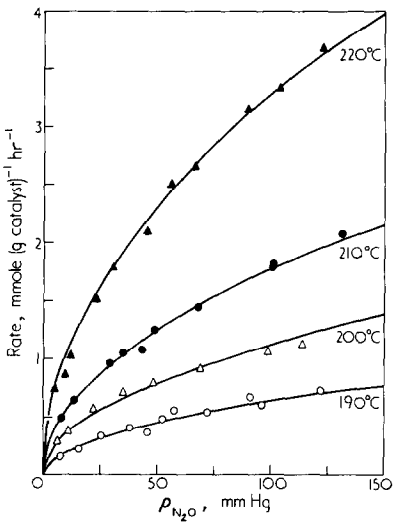

FIG. 2. Effect of p_{N_2O} on CO–N_2O reaction rate on 450°C-activated SnO_2. CO–N_2O–Ar feed at 100 ± 2 cm^3 min^{-1} and constant p_{CO} (275 mm Hg) through 1.0 g bed: (—) plots for rate $= k_2 p_{N_2O}^{0.5}$ for best-fit values of k_2 at each temperature.

Attempts were made to fit theoretical rate equations, derived from Langmuir–Hinshelwood or Rideal–Eley assumptions, according to the method of Hougen and Watson (*12*), to the kinetics data obtained in Figs. 1 and 2, taking into account the following most likely simple reaction mechanisms:

1. Single site mechanisms involving chemisorption of CO or N_2O followed by reaction with gas phase N_2O or CO, respectively.

2. Equivalent and nonequivalent dual site mechanisms involving competitive chemisorption of CO and N_2O on equivalent sites, or selective chemisorption on nonequivalent sites, followed by reaction of adjacent CO and N_2O chemisorbed species.

3. A catalyst redox mechanism involving CO chemisorption, CO_2 desorption via lattice oxygen abstraction, and reoxidation of the catalyst by N_2O.

In view of the absence of product inhibi-

tion, all steps in the above reaction schemes involving desorption of N_2 and CO_2 were considered irreversible in deriving the theoretical equations.

All the derived rate equations could be discarded as inadequately representing the observed experimental data on one of the following two grounds:

a. In the cases where the derived rate equations could be simplified to linear forms (for p_{CO} or p_{N_2O} constant), substitution of the experimental data into the derived rate equations gave obviously nonlinear plots.

b. In the other instances, a linear regression analysis required at least one of the gas adsorption coefficients in the derived rate equation to be large and negative in order to obtain a fit for the experimental data.

In fact, the experimental data were found to be best represented by the empirical relationship:

$$\text{rate} = A \exp(-E/RT) p_{CO}{}^{x} p_{N_2O}{}^{y}, \quad (1)$$

with values of x and y at 190–220°C of between 0.19 and 0.25, and 0.47 and 0.55, respectively.

In all cases, good correlation coefficients (≥ 0.99) were obtained from linear regression analyses of the plots of log rate vs log p_i (i = CO or N_2O at constant p_{N_2O} or p_{CO}, respectively) over the entire gas pressure ranges studied, and the solid curves shown in Figs. 1 and 2 are the best fits obtained after rounding off the CO and N_2O reaction orders to 0.2 and 0.5, respectively. Arrhenius plots for the constants of proportionality (k_1 and k_2 for the data in Figs. 1 and 2, respectively) gave good linear least squares correlation coefficients (0.998 in each case), yielding apparent activation energies of 24.27 (p_{N_2O} constant) and 24.42 (p_{CO} constant) kcal mole^{-1}, respectively.

Thus, the kinetics of the CO–N_2O reaction on 450°C-activated SnO_2 gel are adequately represented by the equation:

$$\text{rate} = A \exp(-E/RT) p_{CO}{}^{0.2} p_{N_2O}{}^{0.5}, \quad (2)$$

with $E = 24.38$ kcal mole^{-1}.

Comparable kinetics studies on 220°C-activated SnO_2 showed a marked similarity with those obtained above for the 450°C-activated catalyst, although the overall reaction rate in the former case was about a factor of 3 higher on a unit weight basis. A similar effect was observed during the air oxidation of CO (*8*), and is attributable to the higher specific surface area of the 220°C-activated material.

Redox Studies

Previous studies on the CO–N_2O reaction on simple oxides (*1–3*) have shown evidence that the reaction occurs by catalyst redox. In addition, where detailed kinetics studies have been undertaken for catalytic oxidations on SnO_2-based catalysts, these have indicated almost exclusively catalyst redox mechanisms. Examples include the oxidation of CO on SnO_2 (*8*), the oxidative dehydrogenation of butenes on tin–antimony oxides (*13,14*), the oxidation of propylene on tin–antimony oxides and tin–phosphorus oxides (*15*), and the oxidation of benzaldehyde (*16*) and *p*-xylene (*17*) on tin–vanadium oxides.

Despite the fact that we have not been able to explain the observed kinetics data for the CO–N_2O reaction on SnO_2 in terms of a catalyst redox mechanism using Langmuir–Hinshelwood assumptions, it was nevertheless thought desirable to investigate the feasibility of the reaction occurring by catalyst redox.

SnO_2 was found to readily undergo successive reduction and reoxidation during CO and N_2O cycling. A typical catalyst reduction ($CatO + CO \rightarrow Cat\square + CO_2$)–reoxidation ($Cat\square + N_2O \rightarrow CatO + N_2$) cycle at 200°C is shown in Fig. 3. The reduction and reoxidation steps were punctuated by flushing with Ar at 200°C for 1–3 hr. This was found to remove most of the residual chemisorbed species and

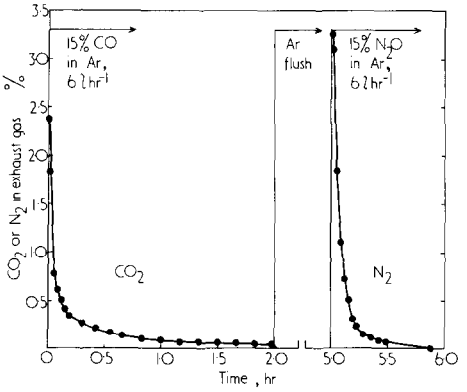

FIG. 3. SnO_2 redox during CO–N_2O cycling at 200°C; 2.0 g bed of 450°C-activated SnO_2.

subsequent thermal desorption studies indicated that about 0.1 cm^3 CO/g and about 1.0 cm^3 N_2O/g (which were almost totally desorbed thermally at 350°C as CO_2 and N_2, respectively) remained on the catalyst after the respective catalyst reductions and reoxidations, followed by flushing with Ar.

During catalyst reduction with CO, the evolved CO_2 was found to tail considerably, indicating that more extensive reduction of the catalyst would occur upon continuation of CO treatment. On the other hand, reoxidation of the catalyst by N_2O was essentially complete within 1 hr.

After taking into account the small contribution due to reaction with the residual chemisorbed species, particularly for the CO reduction steps, the volumes of evolved CO_2 (after 2 hr) and N_2 during the catalyst reduction and reoxidation, respectively, were in good agreement, and after the initial preconditioning cycle, successive cycles gave values of 9–10 cm^3 g^{-1} for these quantities. This corresponds to a maximum degree of reduction equivalent to a value of n in SnO_n of between 1.93 and 1.94, and we have previously indicated (*8*) that, for this catalyst, the reduction can be accounted for by a mechanism of surface oxygen abstraction and does not necessarily demand participation of bulk oxygen. No detectable change in crystal structure accompanies this reduction.

A separate catalyst reoxidation using He instead of Ar as the diluent for N_2O (thus permitting GC detection of molecular oxygen on the molecular sieve column) showed that gaseous oxygen is not produced and thus all the product N_2 is attributable to reoxidation of the catalyst.

The above redox studies have shown that the degree of partial reduction of SnO_2 can be accurately measured by monitoring evolved N_2 after titration with N_2O. This thus affords a method of determining the degree of reduction of steady state SnO_2 after its use in catalyzing the CO–N_2O reaction, and of relating this to the partial pressures of the reactant gases. Thus, two series of experiments were carried out at 200 and 210°C whereby SnO_2 was allowed to establish steady state in various CO–N_2O–Ar mixtures, the steady state reaction rates measured, the system flushed with Ar to remove chemisorbed CO and CO_2 (see above), and then titrated with N_2O over 1 hr to determine the degree of reduction.

The reaction rates and degrees of reduction (θ) were then related to p_{CO} and p_{N_2O} by power law relationships and the best fit values of x, x', y and y' in the expressions:

$$\text{rate} = k_3 p_{CO}{}^{x} p_{N_2O}{}^{y}, \qquad (3)$$

and

$$\theta = k_4 p_{CO}{}^{x'} p_{N_2O}{}^{y'}, \qquad (4)$$

were obtained using linear regression analysis.

The values of 0.2 and 0.5 for x and y, respectively, were again confirmed, and the best fit values for x' and y' were 0.2 and -0.3, respectively. Full details of both series of experiments are shown in Tables 1 and 2, and the observed oxygen deficiences quoted in these tables for the steady state catalysts correspond to values of n in SnO_n of between 1.96 and 1.98.

These data permit the reaction rate to be expressed empirically as a function of θ, i.e.,

$$\text{rate} = k_5 \theta p_{CO}{}^{0.0} p_{N_2O}{}^{0.8}. \qquad (5)$$

TABLE 1
CO–N_2O REACTION RATES AND EXTENTS OF CATALYST REDUCTION AT STEADY STATE AT 200°C[a]

Mean partial pressures (mm Hg)		Rate [mmole (g cat)$^{-1}$ hr^{-1}]		Oxygen deficiency, θ [mg atom (g cat)$^{-1}$]	
p_{CO}	p_{N_2O}	Obsd	Calcd[b]	Obsd[c]	Calcd[d]
164.5	117.5	0.895	0.889	0.135	0.138
46.2	80.3	0.507	0.570	0.122	0.121
83.8	95.1	0.692	0.699	0.132	0.129
265.2	33.5	0.565	0.525	0.205	0.222
100.7	56.8	0.603	0.561	0.153	0.157
22.0	49.6	0.372	0.386	0.131	0.120

[a] CO–N_2O–Ar feeds at 100 ± 2 cm^3 min^{-1} through 1.0 g 450°C-activated SnO_2.
[b] Based on best-fit value of k_3 in equation: rate = $k_3 p_{CO}^{0.2} p_{N_2O}^{0.5}$.
[c] Based on reoxidation capacity of catalyst by N_2O.
[d] Based on best-fit value of k_4 in equation: $\theta = k_4 p_{CO}^{0.2} p_{N_2O}^{-0.3}$.

DISCUSSION

Despite the fact that the observed kinetics of the CO–N_2O reaction on 450°C-activated SnO_2 at 190–220°C cannot be explained in terms of a catalyst redox mechanism using Langmuir–Hinshelwood assumptions, redox studies have yielded strong evidence that the steady state reaction does occur predominantly by such a mechanism. If expressed as a function of the degree of reduction (θ) of the steady state catalyst, then the reaction rate is zero order in p_{CO} and approaches first order in p_{N_2O} [Eq. (5)]. In addition, mathematical treatment (not included here) of the catalyst reoxidation data of Fig. 3 shows that the rate of reduction of N_2O at 200°C as a function of θ can more than account for the rates observed during the steady state CO–N_2O reaction at this temperature (Table 1). This lends further support to the postulate that a catalyst redox mechanism predominates.

The rate of the steady state CO–N_2O reaction on 450°C-activated SnO_2 gel is a factor of about 6 slower than that previously observed for the steady state CO–O_2 reaction under comparable conditions (*8*). Since the latter reaction has been shown to occur by catalyst redox, the rate determining step in the CO–N_2O reaction must be reoxidation of the catalyst by N_2O, based on the redox postulate. The low rate dependence order in p_{CO} compared with that for p_{N_2O} [Eq. (2)] would tend to confirm this, as would the fact that the CO–N_2O reaction has a higher apparent activation energy (24.3 kcal mole^{-1}) compared with that for the CO–O_2 reaction (17.4 kcal mole^{-1}) (*8*) under comparable conditions.

TABLE 2
CO–N_2O REACTION RATES AND EXTENTS OF CATALYST REDUCTION AT STEADY STATE AT 210°C[a]

Mean partial pressures (mm Hg)		Rate [mmole (g cat)$^{-1}$ hr^{-1}]		Oxygen deficiency, θ [mg atom (g cat)$^{-1}$]	
p_{CO}	p_{N_2O}	Obsd	Calcd[b]	Obsd[c]	Calcd[d]
169.7	109.1	1.405	1.460	0.168	0.167
61.8	89.9	1.028	1.083	0.152	0.145
253.4	37.8	0.968	0.932	0.237	0.249
29.8	32.4	0.528	0.562	0.176	0.170
119.1	54.6	1.035	0.962	0.193	0.192
221.4	63.6	1.218	1.176	0.197	0.207

[a–d] As for Table 1.

ACKNOWLEDGMENT

The International Tin Research Council is acknowledged for permission to publish this work.

REFERENCES

1. Schwab, G.-M., and Drikos, J., *Z. Phys. Chem. A*, **186**, 348 (1940).
2. Dell, R. M., Stone, F. S., and Tiley, P. F., *Trans. Faraday Soc.* **49**, 201 (1953).
3. Tanaka, K., and Blyholder, G., *J. Chem. Soc., Chem. Commun.* 736 (1971).
4. Hwang, S. T., and Parravano, G., *J. Electrochem. Soc.* **114**, 482 (1967).
5. Leech, C. A., and Peters, M. S., *AIChE Symp. Ser.* No. 126, **68**, 75 (1972).
6. Shelef, M., and Otto, K., *J. Catal.* **10**, 408 (1968).
7. Fuller, M. J., and Warwick, M. E., *J. Chem. Soc., Chem. Commun.* 210 (1973).

8. Fuller, M. J., and Warwick, M. E., *J. Catal.* **29,** 441 (1973).
9. Fuller, M. J., and Warwick, M. E., *J. Catal.* **34,** 445 (1974).
10. Fuller, M. J., and Warwick, M. E., *J. Chem. Soc., Chem. Commun.* 57 (1974).
11. Andrews, R. H., and Fuller, M. J., unpublished data.
12. Smith, J. M., "Chemical Engineering Kinetics," pp. 202–273. McGraw-Hill, New York, 1956.
13. Bakshi, Y. M., Gur'yanova, R. N., Mal'yan, A. N., and Gel'bshtein, A. I., *Neftekhimiya* **7,** 537 (1967).
14. Trimm, D. L., and Gabbay, D. S., *Trans. Faraday Soc.* **67,** 2782 (1971).
15. Niwa, M., and Murakami, Y., *J. Catal.* **26,** 359 (1972).
16. Sachtler, W. M. H., Dorgelo, G. J. H., Fahrenfort, J., and Voorhoeve, R. J. H., *Proc. Int. Congr. Catal., 4th, 1968,* **1,** 454 (1970).
17. Mathur, B. C., and Viswanath, D. S., *J. Catal.* **32,** 1 (1974).